Journal of Medicinal Chemistry

Article

Lysosomotropism of Basic Cathepsin K Inhibitors Contributes to Increased Cellular Potencies against Off-Target Cathepsins and Reduced Functional Selectivity

Jean-Pierre Falgueyret, Sylvie Desmarais, Renata Oballa, W. Cameron Black, Wanda Cromlish, Karine Khougaz, Sonia Lamontagne, Frederic Mass, Denis Riendeau, Sylvie Toulmond, and M. David Percival

J. Med. Chem., **2005**, 48 (24), 7535-7543• DOI: 10.1021/jm0504961 • Publication Date (Web): 29 October 2005

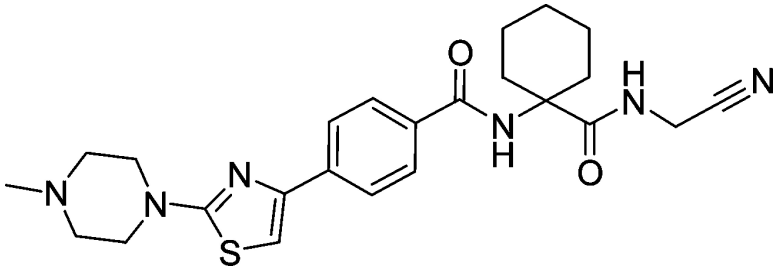

More About This Article

Additional resources and features associated with this article are available within the HTML version:

- Supporting Information
- Links to the 5 articles that cite this article, as of the time of this article download
- Access to high resolution figures
- Links to articles and content related to this article
- Copyright permission to reproduce figures and/or text from this article

View the Full Text HTML

Journal of Medicinal Chemistry is published by the American Chemical Society. 1155 Sixteenth Street N.W., Washington, DC 20036

Lysosomotropism of Basic Cathepsin K Inhibitors Contributes to Increased Cellular Potencies against Off-Target Cathepsins and Reduced Functional Selectivity

Jean-Pierre Falgueyret,[†] Sylvie Desmarais,[†] Renata Oballa,[‡] W. Cameron Black,[‡] Wanda Cromlish,[†] Karine Khougaz,[§] Sonia Lamontagne,[†] Frederic Massé,[†] Denis Riendeau,[†] Sylvie Toulmond,[†] and M. David Percival*,[†]

Departments of Biochemistry, Molecular Biology and Pharmacology, Medicinal Chemistry, and Pharmaceutical Research and Development, Merck Frosst Centre for Therapeutic Research, Kirkland, Quebec, Canada

Received May 26, 2005

The lysosomal cysteine protease cathepsin K is a target for osteoporosis therapy. The aryl-piperazine-containing cathepsin K inhibitor CRA-013783/L-006235 (**1**) displays greater than 4000-fold selectivity against the lysosomal/endosomal antitargets cathepsin B, L, and S. However, **1** and other aryl-piperazine-containing analogues, including balicatib (**10**), are ∼10−100-fold more potent in cell-based enzyme occupancy assays than against each purified enzyme. This phenomenon arises from their basic, lipophilic nature, which results in lysosomal trapping. Consistent with its lysosomotropic nature, **1** accumulates in cells and in rat tissues of high lysosome content. In contrast, nonbasic aryl-morpholino-containing analogues do not exhibit lysosomotropic properties. Increased off-target activities of basic cathepsin K inhibitors were observed in a cell-based cathepsin S antigen presentation assay. No potency increases of basic inhibitors in a functional cathepsin K bone resorption whole cell assay were detected. Therefore, basic cathepsin K inhibitors, such as **1**, suffer from reduced functional selectivities compared to those predicted using purified enzyme assays.

Introduction

Cathepsin K is a member of the papain family of cysteine proteases of which 11 human members have been identified.[1,2] With the exception of cathepsin W, which is localized in the endoplasmic reticulum, all are found in the acidic lysosomal or endosomal compartments of the cell. Certain cysteine cathepsins are also found associated with the cell membrane or are secreted. Cathepsin K is a pharmaceutical target for the treatment of osteoporosis, as it is highly and selectively expressed in osteoclasts, the cells which degrade bone during the continuous cycle of bone degradation and formation.[3] Type I collagen is the major organic constituent of bone, and cathepsin K has a potent collagenase activity, especially at the acidic pH required to destroy the inorganic calcium hydroxyapatite component of bone.

In developing potent and selective cathepsin K inhibitors, most attention has focused on cathepsins B, L, and S as antitargets, as they have high degrees of homology to cathepsin K and have been attributed important functions in vivo.[4−6] Inhibitory potencies against target and antitarget cathepsins are generally determined using purified enzymes at the optimal acidic pH for each enzyme and can give reliable estimates of intrinsic potencies. However, these assay conditions may not always reflect those of the enzyme in the cell, due to differences in pH, ionic strength, presence of other proteins and membranes, and cellular permeability. On the other hand, the absence of highly specific endogenous or peptide substrates to measure the cellular activities of individual cathepsins has hindered the development of whole cell cathepsin assays. More recently, whole cell enzyme occupancy assays have been used to determine cathepsin inhibitor potencies within intact cells. These assays employ a radiolabeled irreversible inhibitor which competes with the reversible test compound for the active site of the target enzyme.[7,8]

The successful targeting of a cathepsin K inhibitor to lysosomes by conjugation with poly(ethylene glycol) polymers has been described.[9] These conjugated inhibitors enter the cell by endocytosis, leading to lysosomal drug delivery. Lysosomotropism, which is defined as the ability of compounds to accumulate in acidic compartments, is also a property of weakly basic, lipophilic molecules.[10] Neutral species are able to freely diffuse across the cell membrane, but become membrane impermeable once protonated within the acidic compartment. The degree of compound accumulation is dependent on its pK_a and the pH difference between the cytosol and the lysosome. In addition, compound lipophilicity can affect lysosomal accumulation, due to aggregation or interaction with lipid membranes.[11,12] Many common drugs are highly lysosomotropic, and this property has often been linked, especially in animal safety studies, to the development of phospholipidosis.[13] Drug lysosomotropism may also result in an alteration of the disposition of other basic compounds[14] and has also been linked to the formation of lysosomal lipofuscin-like bodies.[15]

* Correspondence to M. David Percival, Department of Biochemistry and Molecular Biology, Merck Frosst Centre for Therapeutic Research, P.O. Box 1005, Pointe-Claire-Dorval, Quebec, Canada. H9R 4P8. Tel 514-428-3191. Fax 514-428-4930. E-mail: dave_percival@merck.com.
[†] Department of Biochemistry, Molecular Biology and Pharmacology.
[‡] Department of Medicinal Chemistry.
[§] Department of Pharmaceutical Research and Development.

10.1021/jm0504961 CCC: $30.25
Published on Web 10/29/2005

Scheme 1. Synthesis of Compound **2**

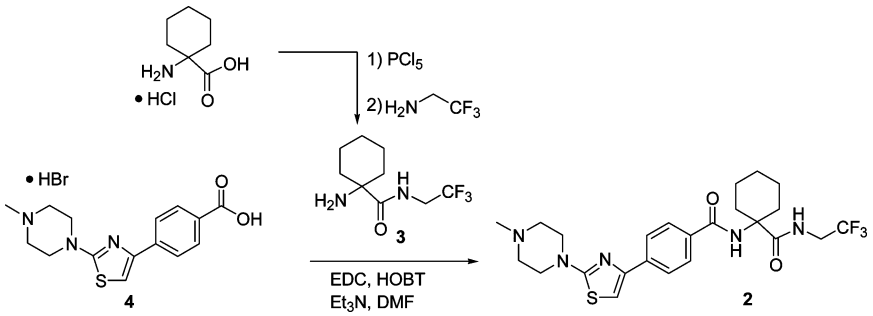

Scheme 2. Synthesis of ^{14}C-**1**

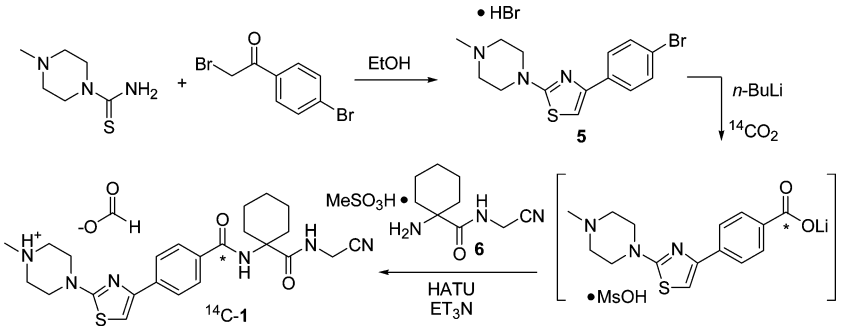

Scheme 3. Synthesis of ^{14}C-**9**

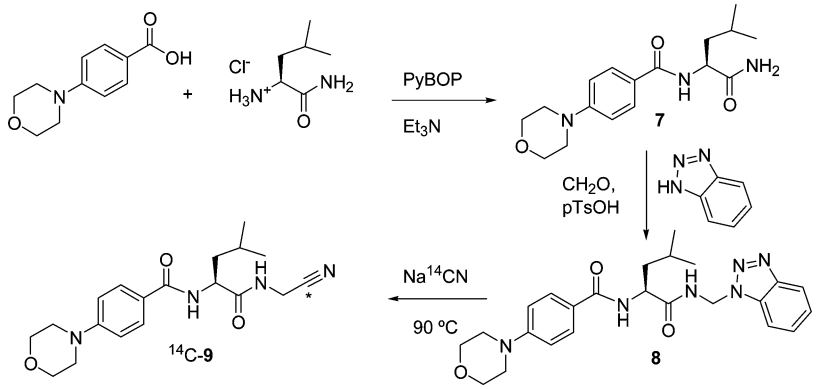

Here we describe examples of basic amine-containing cathepsin K inhibitors which show lysosomotropic behavior. This feature of these inhibitors has important consequences for their activities against antitargets as well as their tissue distributions.

Biochemistry. The conditions used to assess inhibitor potencies against purified human cathepsins B, L, and S and rabbit cathepsin K, as well as the whole cell enzyme occupancy assays for human cathepsins B (in HepG2 cells), L (in HepG2 cells), and S (in Ramos cells), were previously described.[8] The effects of buffer pH on inhibitor potencies against cathepsins B, K, L, and S were performed using constant ionic strength buffers (50 mM) at pH 3.5 and 4.5 (formate), pH 5.5 (acetate), and pH 6.5 and 7.5 (Bis-Tris). Ionic strength was adjusted with NaCl. Buffer additives for each cathepsin were as previously detailed.[8] The enzyme assay for mouse cathepsin S[16] was performed under the same conditions as that for the human enzyme. The rabbit osteoclast bone resorption assay was also previously described.[17]

Chemistry. The synthesis of the non-nitrile **2** is described in Scheme 1. Trifluoroethylamine is reacted with 1-aminocyclohexanecarbonyl chloride to generate the amine **3** which is then coupled with the acid **4** [18] under amide bond forming conditions to afford **2**, the non-nitrile version of **1**.

The synthesis of the radiolabeled cathepsin inhibitor ^{14}C-**1** involves the lithiation of the aryl bromide **5** with *n*-BuLi and trapping of the resultant aryllithium with $^{14}CO_2$ (Scheme 2). The final step is an amide bond formation with HATU and 1-amino-*N*-(cyanomethyl)-cyclohexanecarboxamide methanesulfonate (**6**).[18]

The synthesis of the nonbasic radiolabeled cathepsin inhibitor ^{14}C-**9** involves the reaction of amide **7** with formaldehyde and benzotriazole (Scheme 3). The resultant benzotriazole **8** is then treated with Na^{14}CN at 90 °C which affords ^{14}C-**9**.

Results and Discussion

We recently described the synthesis and biological activities of the potent, reversible inhibitor of cathepsin K, CRA-013783/L-006235 (**1**) (Figure 1).[19a] On the basis of inhibitory potencies against purified human cathepsins, **1** is highly active against human cathepsin K (IC_{50} ~0.25 nM) and is over 4000-fold selective against

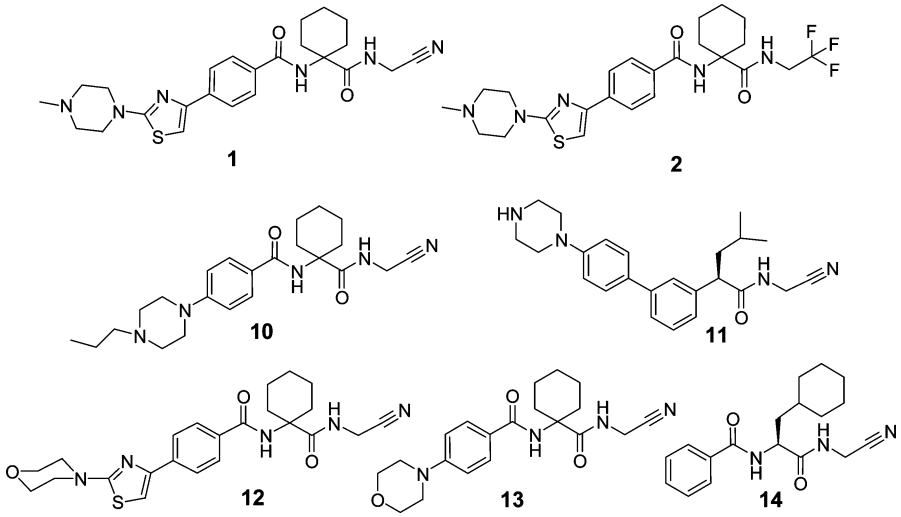

Figure 1. Structures of cathepsin inhibitors used in this study.

Table 1. Potencies for Basic and Nonbasic Cathepsin K Inhibitors Inhibitors against Humanized Rabbit Cathepsin K,[20] Human Cathepsins B, L, and S in Purified Enzyme and Whole Cell Enzyme Occupancy Assays[a]

	inhibition of cathepsins, IC_{50} (nM)						
	Cathepsin K	Cathepsin B		Cathepsin L		Cathepsin S	
	enzyme	enzyme	cell (HepG2)	enzyme	cell (HepG2)	enzyme	cell (Ramos)
(**1**)	0.25[19]	1100 ± 43	17 ± 3	6300 ± 1500	340 ± 35	47000 ± 7000	790 ± 420
(**10**)	1.4 ± 0.4	4800 ± 200	61 ± 22	503 ± 80	48 ± 15	65000 ± 4000	2900 ± 1300
(**11**)	7.8 ± 0.8	86000 ± 14000	4400 ± 2000	2600 ± 250	320 ± 170	20000 ± 7000	1340 ± 400
(**12**)	2.3 ± 0.04	4200 ± 500	2900 ± 1100	24000 ± 3000	>10000	27000 ± 3000	>10000
(**13**)	19 ± 6	15400 ± 1000	4400 ± 1900	32000 ± 6000	>10000	52000 ± 6000	4800 ± 2600
(**14**)	1030 ± 308	19000 ± 4000	940 ± 370	55 ± 11	230 ± 180	5.3 ± 0.2	10 ± 6

[a] The data represent averages (±SEM) of at least duplicate experiments.

cathepsins B, L, and S (Table 1). However, when tested in human whole cell enzyme occupancy assays against cathepsins B, L, and S, it is apparent that the potencies against these enzymes in their native cellular environment are increased ~20−60-fold (Table 1). Other piperazine-thiazole analogues (which had modifications at the P2 spirocyclohexyl group, data not shown), as well as a *N*-propyl-piperazine analogue **10** (balicatib)[19a,b] and a nonpeptidic biaryl piperazine-containing cathepsin K inhibitor **11**,[20] were also significantly more potent in cell-based assays than against purified cathepsins (Table 1). In contrast, analogues of these compounds containing a morpholino or a phenyl functionality (**12**, **13**, and **14**),[18,19a] generally gave similar IC_{50} values in both cell and purified enzyme assays for each cathepsin (Table 1).

The above observations suggest that the purified enzyme assay conditions for cathepsins B, L, and S do not reflect the cellular enzyme environment, resulting in inhibitor potencies for compounds **1**, **10**, and **11** (but not **12**, **13**, and **14**) which do not match those obtained in whole cells. This phenomenon may be due to the basic piperazine-containing compounds **1**, **10**, and **11** concentrating in the acidic lysosomal/endosomal compartments containing the target cathepsins, a process known as lysosomotropism. Alternatively, the differences in cellular and enzyme potencies of **1**, **10**, and **11** may be related to pH-dependent differences in the piperazine group protonation state of these inhibitors.[21] This may lead to pH-dependent changes in inhibitor potencies that do not correspond to those found with neutral inhibitors. However, the titration of compounds **1**, **10**, **11**, **12**, **13**, and **14** against purified cathepsins B, K, L, and S over the pH range 3.5 to 7.5 revealed only small decreases in inhibitory potencies at both pH extremes (≤4-fold), as compared to the potencies determined under the conditions used in Table 1 (pH 5.5 to 6.5). In no cases were inhibitor potencies significantly increased over the pH range 3.5 to 7.5 compared to those obtained at pH 5.5 to 6.5, consistent with previous studies.[21]

The piperazine-thiazole-phenyl group of **1** is intrinsically fluorescent which enabled its subcellular distribution to be examined in whole live cells by two-photon confocal microscopy. Following incubation with 10 μM **1** for 1 h, HepG2 cells show a punctate fluorescence throughout the cytoplasm (Figure 2A). A similar pattern and intensity of cellular fluorescence was obtained with the analogue **2**, in which the electrophilic aminoacetonitrile warhead, which forms a thioimidate linkage with the active site cysteine, is replaced by an unreactive trifluoroethylamino group (Figure 2B). Compound **2** is devoid of activity against cathepsins B, L, K, and S (IC_{50} > 10 μM), demonstrating that the accumulation of **1** within the cell is not due to binding to cysteine cathepsins or other activated thiol-containing proteins. Little cellular autofluorescence was observed with vehicle-treated cells (Figure 2C). The cellular fluorescence was blocked when cells were pretreated with 10 mM NH_4Cl which causes the alkalinization of acidic subcellular compartments (data not shown).[22] The punctate cytosolic fluorescence obtained with **1** colocalizes with that of the fluorescent lysosomal probe LysoTracker Red DND-99 (Figure 2D−F). Similar results were obtained with human umbilical vein endothelial cells, another cell

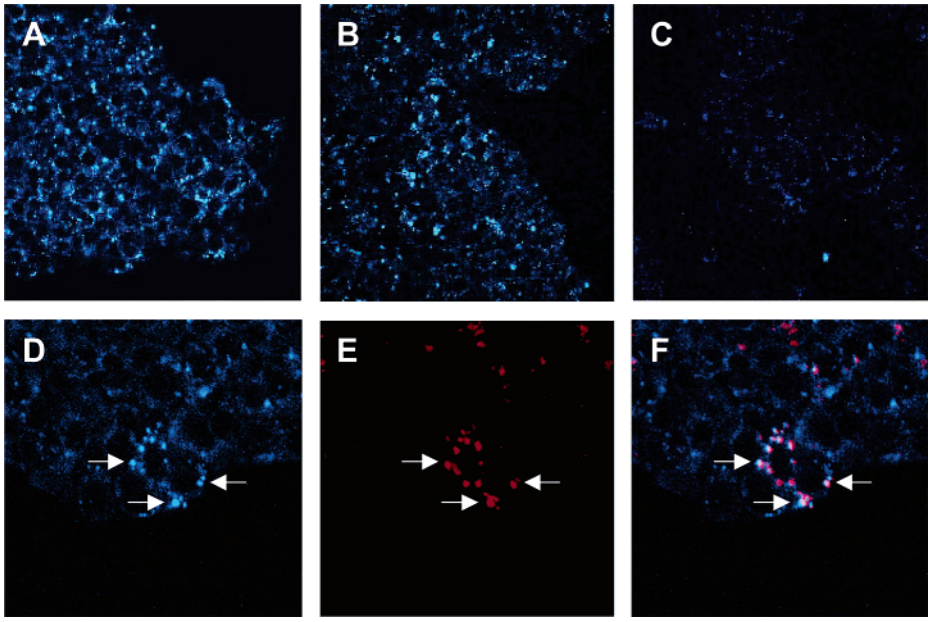

Figure 2. Accumulation of **1** within lysosomes of HepG2 cells as observed by two-photon confocal microscopy. HepG2 cells were incubated for 1 h with 10 μM of either **1** (A) or **2** (B) or DMSO vehicle (C) (all measured at an original magnification of 20×). To assess the accumulation of **1** in lysosomes, colocalization with LysoTracker Red DND-99 was performed. The figures show fluorescence observed with either **1** (D) or Red DND-99 (E) and when the two images are merged (F). Arrows indicate lysosomes containing both **1** and Red DND-99 (original magnification 20×).

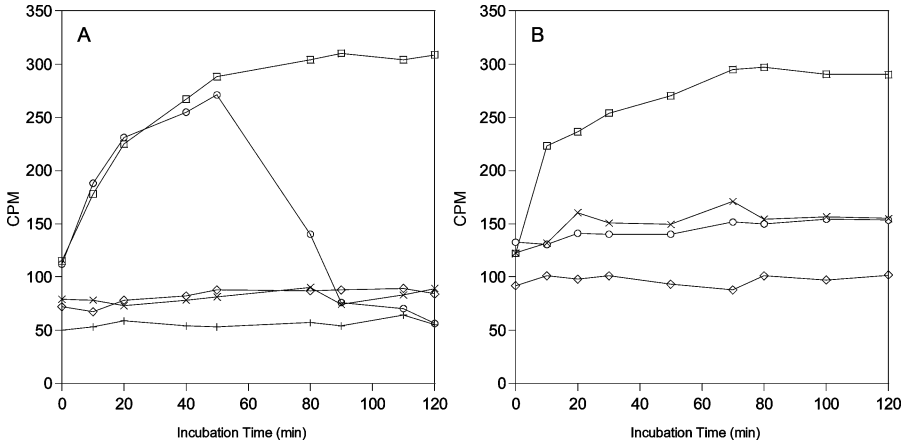

Figure 3. Accumulation of ^{14}C-labeled cathepsin K inhibitors in HepG2 cells. A: HepG2 cells were grown to ~90% confluency in a Cytostar-T scintillation microplate and were incubated at time −10 min with 30 μM (0.02 μCi) ^{14}C-**1** (□) or 30 μM (0.02 μCi) ^{14}C-**9** (×), prior to determination of the accumulation of compound in cells by scintillation counting. After 50 min incubation, the media containing ^{14}C-**1** was replaced by media without compound (○). Controls were performed without cells in the presence of 30 μM ^{14}C-**1** (◇) and 30 μM ^{14}C-**9** (+). B: HepG2 cells were incubated in the presence of 30 μM of ^{14}C-**1** alone (□), after a 2 h preincubation with 10 μM monensin (○), or after a 2 h preincubation with 10 mM NH_4Cl (×). Control without cells in the presence of 30 μM ^{14}C-**1** (◇).

type which contains large numbers of lysosomes. Compounds **12** and **13** do not have an appropriate intrinsic fluorescence, therefore precluding similar cell-based studies with these nonbasic, morpholino-containing cathepsin K inhibitors.

The accumulation of piperazine and morpholino-containing cathepsin K inhibitors in cells was further investigated using ^{14}C-labeled **1** and **9** (Schemes 2 and 3). HepG2 cells were grown as a monolayer in the wells of a Cytostar-T scintillation microplate. Either ^{14}C-labeled **1** or **9** (30 μM) were added to the cell media, and the signal, resulting from collision of the short travelling β-particles with the scintillant in the base of the plate, was determined over time. A signal is only produced when β-particles are emitted in close proximity to the plate base, i.e., associated with attached cells and not when β-particles are emitted in the media above the cells. The radioactivity signal from ^{14}C-labeled **1** increased rapidly over the first 40 min of the incubation with the cells and then was constant until 120 min (Figure 3A). In contrast, no time-dependent signal increase was observed with the morpholino-containing ^{14}C-labeled **9** in the presence of HepG2 cells, and the signal obtained was similar to that of ^{14}C-labeled **1** and **9** in the absence of cells. The apparent accumulation of ^{14}C-**1** in the HepG2 cells was reversible, since replacement with fresh media (not containing ^{14}C-**1**) after an incubation time of 50 min resulted in a rapid loss of signal (Figure 3A). The uptake of ^{14}C-**1** into the cells was not saturated at 30 μM, as the incubation with 60 μM ^{14}C-**1** resulted in an approximate doubling of both the rate of signal increase and the maximal intensity

Table 2. Experimentally determined Piperazine Group pK_a and Log *P* Values of Cathepsin K Inhibitors

	Log *P*	pK_a
(**1**)	2.30 ± 0.04	7.01 ± 0.05
(**2**)	2.9 ± 0.3	6.84 ± 0.03
(**10**)	1.81 ± 0.05	7.76 ± 0.05
(**11**)	3.46 ± 0.03	8.77 ± 0.03
(**13**)	0.98 ± 0.03	–

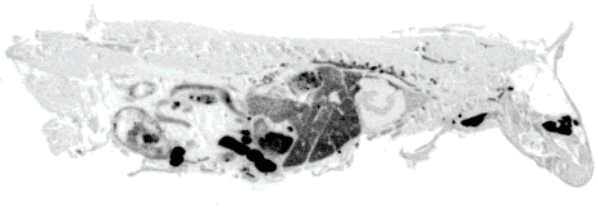

Figure 4. Whole-body autoradiogram illustrating the distribution of ^{14}C-**1** in the female Sprague–Dawley rat. ^{14}C-**1** whole-body distribution was assessed 1 h after iv injection of the radiolabeled compound.

Table 3. Rat Whole Body Distribution of ^{14}C-**1**[a]

tissue	concn (μM)	tissue	concn (μM)
small intestine content	289	spinal marrow	15
bladder content	148	thyroid	14
salivary glands	54	bone marrow	11
lung	49	large intestine content	9
lachrymal glands	45	thymus	6
liver	26	heart	6
spleen	23	pancreas	5
adrenal glands	22	muscle	4
brown fat	21	blood	4
pituitary	19	white fat	2
kidney	15	brain	1

[a] Tissue concentrations were determined by analysis of whole body sections 1 h following an iv dose using β Vision$^+$ software.

(data not shown). The pretreatment of the HepG2 cells with either monensin or NH_4Cl, both agents which result in the alkalinization of lysosomes, inhibited the time dependent signal increase obtained with ^{14}C-**1** (Figure 3B).

The above data is consistent with the aryl-piperazine groups of **1**, **10**, and **11** conferring lysosomotropic properties on these cathepsin K inhibitors, thus providing them with increased lysosomal concentrations and, in turn, increased apparent whole cell potencies. The experimentally determined pK_a and Log *P* values of the cathepsin inhibitors (Table 2) reveal that **1**, **2**, **10**, and **11** have pK_a values around neutrality or higher and are relatively lipophilic, two features required for a high degree of lysosomotropism.[11] The calculated pK_a values, by ACD software, for the terminal piperazine nitrogen of **1**, **2**, **10**, and **11** gave values ranging from 6.1 to 8.9. By comparison, the nitrogen proximal to the aromatic group gave calculated pK_a values in the range of −1.3 to 2.2 for these four compounds. A second experimental pK_a value of 1.76 ± 0.22 was obtained for **11** (calculated value 2.2 ± 0.4), consistent with the above assignment.

A study of the whole body distribution of ^{14}C-**1** in rats by autoradiography (Figure 4, Table 3) 1 h after iv injection of the radiolabeled compound showed high concentrations in the liver, kidney, and small intestine and urinary bladder contents, indicating that ^{14}C-**1** is rapidly eliminated via the biliary and renal excretion routes. The whole body distribution study identified other organs, including lung, spleen, and salivary, lachrymal, adrenal, pituitary, and thyroid glands as other sites of accumulation of **1** and/or its metabolites. Low concentrations of radioactivity were detected in the muscle and white fat.

Rat tissue distribution studies further confirmed the accumulation of the parent compound **1** in kidney, spleen, lung and liver, and showed that concentrations of both **1** and **10** in these tissues are ∼6−12 times greater than those found in plasma (Table 4). These tissues have high lysosome contents and are well-known as the sites of concentration of lysosomotropic drugs.[23,24] In contrast, the concentrations of **1** and **10** in white fat and muscle, two tissues with low lysosome contents, are similar to their plasma concentrations. The nonbasic inhibitor **13** does not show any accumulation in tissues with high lysosome content, and the tissue concentrations in liver, kidney, and lung are similar to that in plasma (Table 4). In general, lysosomotropic drugs have a high volume of distribution (V_d) and have tissue levels higher than that in plasma. The V_d of **1** is ∼2-fold higher than that of **10** which may be related to its higher Log *P* value (Table 2), whereas the V_d of **13** is close to unity. The lysosmotropic properties of **1** may contribute to its favorable pharmacokinetic profile, as its terminal half-life is increased 7-fold over that of the morpholino analogue **12**.[19a]

The possibility was considered that the lysosomotropic properties of **1** may also contribute to its functional efficacy, since cathepsin K-mediated degradation of collagen occurs in the acidic lacunae between the osteoclasts and bone, as well as in lysosomes within the osteoclasts.[25,26] Thus, one may expect the increased potencies of basic compounds such as **1**, **10**, and **11** against antitarget cathepsins B, L, and S in whole cell assays (Table 1), to be compensated by a corresponding increased potency against cellular cathepsin K activity. However, a comparison of the potencies of basic and nonbasic inhibitors against purified rabbit cathepsin K with those from a functional rabbit osteoclast bone resorption assay does not confirm this prediction (Table 5). Although the intrinsic potencies of the basic compounds **1** and **10** against rabbit cathepsin K are greater than their nonbasic analogues **12** and **13** (due to a favorable electrostatic interaction with a S3 aspartic acid),[19a] the potency shifts between the purified enzyme assay and the functional cell-based assay are roughly equivalent for both basic and nonbasic inhibitors. It should be emphasized that the cathepsin K bone resorption assay is a functional assay that measures type I collagen degradation after a three day incubation of osteoclasts and bone with test compound. The IC_{50} value from the osteoclast assay for a given compound should not therefore be directly compared with those from the cathepsins B, L, and S whole cell assays, which measure the degree of inhibitor occupancy of the active site of each enzyme in their native cellular environments. Although whole cell enzyme occupancy inhibitor potencies may not be equivalent to those obtained in functional assays, the same rank order of potencies would be expected for a series of inhibitors in the two types of assays.

Table 4. Drug Tissue Concentrations in Rats[a]

compound	tissue concentration (μM)								V_d (L/kg)
	liver	kidney[b]	lung	spleen	muscle	brain	fat	plasma	
1[c]	20	15	16	20	5	1.1	_	2.4	11
10[c]	37	41	31	35	5	0.6	2.5	3.6	4.7
13[d]	0.18	0.22	0.18	–	0.22	0.02	0.03	0.17	1.9

[a] Compounds were dosed either po or iv and tissues taken for analysis 2 h following dosing. [b] Renal cortex. [c] Dosed at 10 mg/kg po. [d] Dosed at 5 mg/kg iv.

Table 5. Shift in Inhibitor Potencies between Rabbit Cathepsin K Enzyme Assay and Functional Rabbit Bone Resorption Assay for Basic and Nonbasic Inhibitors[a]

	inhibition of cathepsin K, IC_{50} (nM) (±SEM)		
	rabbit cathepsin K	rabbit bone resorption assay	potency shift (fold)
(**1**)	0.5	5 ± 1	10
(**10**)	2.7 ± 0.6	97 ± 6	35
(**11**)	33 ± 2	149 ± 20	5
(**12**)	9.5 ± 0.6	41 ± 12	4
(**13**)	72 ± 27	580 ± 230	8

[a] The data represent averages (±SEM) of at least duplicate experiments.

Table 6. Potencies for Basic and Nonbasic Cathepsin K Inhibitors against Mouse Cathepsin S in Purified Enzyme, Whole Cell Mouse Splenocyte Enzyme Occupancy, and Cell-based Functional Mouse Antigen Presentation Assays[a]

	inhibition of mouse cathepsin S, IC_{50} (nM) (± SEM)		
	enzyme	cell (splenocyte)	antigen presentation
(**1**)	5400 ± 150	318 ± 150	6200 ± 1800
(**2**)	33000 ± 5000	>10000	>100000
(**10**)	6350 ± 180	480 ± 100	6180 ± 1400
(**11**)	34100 ± 500	740 (n=1)	8600 ± 5000
(**12**)	8500 ± 3000	6700 ± 900	>100000
(**13**)	4500 ± 900	8500 ± 1500	>100000
(**14**)	13 ± 4	40 ± 18	1220 ± 300

[a] The data represent averages (±SEM) of at least duplicate experiments (except where noted).

The effect of inhibitor basicity on off-target cathepsin S functional activity was investigated using a cell-based mouse antigen presentation assay (Table 6). In a subset of antigen-presenting cells, cathepsin S cleaves the invariant chain (Ii) to allow efficient peptide antigen loading of the type II major histocompatibility complex and antigen presentation.[27] The nonbasic cathepsin S selective inhibitor **14**,[28] which is highly potent in both purified mouse cathepsin S enzyme and mouse splenocyte whole cell cathepsin S enzyme occupancy assays, is significantly shifted to lower potency in the cell-based functional assay of antigen presentation. In contrast, the basic inhibitors (**1**, **10**, and **11**), which are relatively weak against purified mouse cathepsin S (but show increased activity in the splenocyte whole cell enzyme occupancy assay) exhibit unexpected activities in the cathepsin S-dependent cell-based antigen presentation assay. Cathepsin K is not known to play a role in antigen presentation. These results suggest that the lysosomotropic properties of **1**, **10**, and **11** contribute to their potencies in the functional cell-based assay. By comparison, the neutral analogues **12** and **13**, which have similar potencies to **1**, **10**, and **11** against purified mouse cathepsin S, are inactive in the functional assay. The mouse splenocyte cathepsin S enzyme occupancy assay results (Table 6) are consistent with those obtained in human Ramos cells (Table 1) and show increased cellular potencies for the basic nitrogen-containing inhibitors alone. A possible additional functional effect of lysosomal/endosomal alkalinization does not appear to be a major contributor to the potency of the basic compounds, as **2** (which is basic, but only weakly active versus isolated cathepsins) is inactive in the functional cathepsin S assay. The requirement for a high degree of cathepsin S inhibition for functional activity by the potent, neutral inhibitor **14**, is consistent with observations of cathepsin S genetic deletion in mice. In these animals, the cathepsin S substrate Ii p10 accumulates in splenocytes of homozygous null mice, but not to any detectable degree in heterozygotes.[29] Although the potencies of the basic cathepsin K inhibitors (**1**, **10**, and **11**) in the functional cathepsin S antigen presentation assay are relatively weak, it demonstrates the affect of their accumulation in the acidic subcellular compartment that contains an antitarget enzyme. It is expected that lysosomal cathepsin B activity would be inhibited by relatively low concentrations of **1**, **10**, and **11**, as predicted by the potencies of these compounds in the cathepsin B whole cell enzyme occupancy assay (Table 1).

Conclusion

In summary, we have demonstrated that the basic nitrogen-containing lipophilic cathepsin K inhibitors described here exhibit lysosomotropic properties. This feature results in their accumulation within acidic subcellular organelles and an apparent increase in inhibitor potency against the antitarget enzymes present in these compartments. Interestingly, their lysosomotropic properties do not result in increased potencies in a functional cathepsin K assay of bone resorption, but do so against the antitarget cathepsin S. The reason for this anomaly is unknown, but practically, this results in a reduction in the effective selectivity of these basic inhibitors. This phenomenon of increased potency of basic compounds against lysosomal cathepsins is not likely a cathepsin-specific effect and should manifest itself for other lysosomal targets as well. Thus, the cellular potencies of lysosomotropic inhibitors which selectively target lysosomal cathepsins (e.g. B, L, and S) would be predicted to be increased over those determined using purified enzymes. The techniques described here, as well as others in the literature,[11,22] should facilitate the identification of lysosomotropic molecules and aid in the understanding of the inhibition of their targets in their native subcellular compartments.

Experimental Section

General. Proton (^{1}H NMR) magnetic resonance spectra were recorded on a Bruker instrument operating at either 400 or 500 MHz. All spectra were recorded using residual solvent (DMSO or acetone) as internal standard. Signal multiplicity was designated according to the following abbreviations: s =

singlet, d = doublet, dd = doublet of doublets, t = triplet, m = multiplet, br s = broad singlet. Elemental analyses were provided by Onieda Research Services Inc., Whitesboro, NY. High-resolution mass spectra (HRMS−FAB$^+$) were obtained at the Biomedical Mass Spectrometry Unit, McGill University, Montreal, Quebec, Canada. All substrates and reagents were obtained commercially and used without further purification. Reactions were carried out with continuous stirring under a positive pressure of nitrogen except where noted. Flash chromatography was carried out with silica gel 60, 230−400 mesh. Compounds **1**, **10**, **11**, **12**, **13**, and **14** were prepared as previously described.[19a,20,28]

4-[2-(-Methylpiperazin-1-yl)-1,3-thiazol-4-yl]-*N*-(1-{[(2,2,2-trifluoroethyl)amino]-carbonyl}cyclohexyl)benzamide (2). To a solution of PCl_5 (27.6 g, 132 mmol) in CH_3CN (400 mL) was added 1-aminocyclohexanecarboxylic acid hydrochloride (20 g, 111 mmol). The resultant slurry was stirred at room temperature for 3 h followed by filtration. The filter cake was washed with CH_3CN and dried under a N_2 flow followed by drying under high vacuum overnight. 1-Aminocyclohexanecarbonyl chloride hydrochloride was obtained in 91% yield (20 g). To a mixture of 1-aminocyclohexanecarbonyl chloride hydrochloride (10.2 g, 51.5 mmol) in CH_3CN (400 mL) was added trifluoroethylamine (9.0 mL, 113 mmol) over 5 min. The resultant slurry was stirred at room temperature for 30 min before partitioning between EtOAc and water. The organic layer was separated, dried over $MgSO_4$, and concentrated to yield 1-amino-*N*-(2,2,2-trifluoroethyl)cyclohexane-carboxamide (**3**) (7.79 g, 67% yield) which was used as such in the next reaction. ^{1}H NMR (acetone-d_6, 500 MHz) δ 8.45 (1H, br s), 3.42 (2H, m), 1.85 (3H, m), 1.59 (4H, m), 1.38 (2H, br d), 1.25 (1H, m).

To a solution of 4-[2-(4-methylpiperazin-1-yl)-1,3-thiazol-4-yl]benzoic acid hydrobromide (**4**)[18] (13.42 g, 34.9 mmol) and the amine **3** (7.79 g, 34.7 mmol) in DMF (65 mL) were added Et_3N (12.1 mL, 86.8 mmol), HOBT·H_2O (5.58 g, 36.4 mmol), and EDC·H_2O (7.3 g, 38.1 mmol). The reaction mixture was stirred at room temperature for 2 days and then partitioned between EtOAc and water. The organic layer was separated, dried over Na_2SO_4, and concentrated. The resultant beige solid was stirred with boiling EtOAc (400 mL) followed by the addition of hexane (400 mL). A light beige solid was collected by filtration to afford 4-[2-(4-methylpiperazin-1-yl)-1,3-thiazol-4-yl]-*N*-(1-{[(2,2,2-trifluoroethyl)amino]-carbonyl}cyclohexyl)-benzamide (**2**) (7.89 g, 45% yield). The product was determined to be >99.5% pure by reverse phase HPLC. ^{1}H NMR (acetone-d_6, 500 MHz) δ 7.97 (2H, d), 7.95 (1H, m), 7.91 (2H, d), 7.43 (1H, br s), 7.23 (1H, s), 3.94 (2H, m), 3.52 (4H, t), 2.48 (4H, t), 2.29 (2H, m), 2.27 (3H, s), 1.94 (2H, m), 1.62 (5H, m), 1.35 (1H, m). HRMS (+FAB): calcd for $C_{24}H_{31}N_5O_2SF_3$ [MH+] 510.21528, found 510.21506. Anal. ($C_{24}H_{30}N_5O_2SF_3$) C: calcd, 56.57; found, 56.04; H: calcd, 5.93; found, 5.25; N: calcd, 13.74; found, 13.59; S: calcd, 6.29; found, 6.13.

^{14}C-*N*-(1-{[(Cyanomethyl)amino]carbonyl}cyclohexyl)-4-[2-(4-methylpiperazin-1-yl)-1,3-thiazol-4-yl]benzamide (^{14}C-1). To a suspension of 2-bromo-1-(4-bromophenyl)-ethanone (1.96 g, 7.05 mmol) in EtOH (50 mL) was added 4-methylpiperazine-1-carbothioamide (1.12 g, 7.03 mmol). The mixture was heated to reflux for 1.5 h, then cooled and filtered to give 2.82 g (95%) of 4-[4-(4-bromophenyl)-1,3-thiazol-2-yl]-1-methylpiperazin-1-ium bromide. ^{1}H NMR (DMSO-d_6, 400 MHz) δ 9.9 (1H, br s), 7.82 (2H, d), 7.60 (2H, d), 7.48 (1H, s), 4.1 (2H, br s), 3.5 (2H, br s), 3.4 (2H, br s), 3.2 (2H, br s), 2.85 (3H, s). This salt (585 mg) was partitioned between ethyl acetate and aq $NaHCO_3$. The organic phase was washed with brine, dried over $MgSO_4$ and evaporated to give 400 mg of 1-[4-(4-bromophenyl)-1,3-thiazol-2-yl]-4-methylpiperazine (**5**). ^{1}H NMR (DMSO-d_6, 400 MHz) δ 7.80 (2H, d), 7.55 (2H, d), 7.35 (1H, s), 3.45 (4H, m), 2.43 (4H, m), 2.21 (3H, s).

To a −78 °C solution of 1-[4-(4-bromophenyl)-1,3-thiazol-2-yl]-4-methylpiperazine (**5**) (195 mg, 0.576 mmol) in THF (8 mL) was added *n*-BuLi (1.6 M, 0.43 mL, 0.69 mmol), and the solution was stirred for 15 min. A cannula was connected between this flask and a 5 mL flask containing $Ba^{14}CO_3$ (114 mg, 3.6 mCi/mmol), and both flasks were swept with N_2(g). The aryllithium flask was cooled in liquid nitrogen and the N_2 (g) flow was stopped when the solvent solidified. Concentrated sulfuric acid (0.8 mL) was then added dropwise to the $Ba^{14}CO_3$, liberating $^{14}CO_2$. After 5 min, both the cannula and the liquid nitrogen bath were removed, and the flask was allowed to warm to −78 °C and stir for 1 h. The mixture was then warmed to room temperature, where TLC analysis indicated formation of lithium 4-[2-(4-methylpiperazin-1-yl)-1,3-thiazol-4-yl]benzoate. The THF was removed under a flow of N_2 (g). To the residue were added HATU (220 mg, 0.58 mmol), 1-amino-*N*-(cyanomethyl)cyclohexanecarboxamide methanesulfonate (**6**)[18] (167 mg, 0.60 mmol), and DMF (4 mL). Triethylamine (0.1 mL, 0.7 mmol) was then added, the mixture was stirred overnight at room temperature and then partitioned between ethyl acetate and water. The organic phase was washed with dilute $NaHCO_3$ and brine and then dried over Na_2SO_4 and concentrated. The experiment was repeated with 267 mg of 1-[4-(4-bromophenyl)-1,3-thiazol-2-yl]-4-methylpiperazine (**5**), and the combined crude products were purified by flash chromatography (5 to 7% MeOH in CH_2Cl_2 + 0.5% NH_4OH) to give 155 mg of 92% pure ^{14}C-*N*-(1-{[(cyanomethyl)amino]carbonyl}cyclohexyl)-4-[2-(4-methylpiperazin-1-yl)-1,3-thiazol-4-yl]benzamide (^{14}C-**1**). Further purification was accomplished using preparative HPLC (RP C18 column, gradient: 27% to 31% CH_3CN/0.2% aq formic acid over 10 min, T_R = 4.4 min) to provide 101 mg of the title compound (0.197 mmol, 0.71 mCi).

^{14}C-*N*^{1}-(Cyanomethyl)-*N*^{2}-(4-morpholin-4-ylbenzoyl)-leucinamide (^{14}C-9). To a solution of 4-morpholin-4-ylbenzoic acid (0.73 g, 1 equiv) and PyBOP (1.6 g, 1 equiv) in DMF (25 mL) was added triethylamine (1.3 mL, 3.1 equiv). The reaction mixture was stirred at room temperature for 10 min followed by the addition of L-leucinamide hydrochloride (0.5 g, 1 equiv). The resultant suspension was stirred at room temperature under an atmosphere of nitrogen overnight. Saturated aqueous $NaHCO_3$ was added followed by EtOAc and water. The aqueous layer was separated and extracted with EtOAc (7×). The combined organic extracts were washed with water (1×), dried, and concentrated. The residue was stirred with a minimal amount of diethyl ether and then filtered to provide 0.91 g (95% yield) of the desired *N*^{2}-(4-morpholin-4-ylbenzoyl)-leucinamide (**7**). ^{1}H NMR (400 MHz, DMSO-d_6) δ 8.05 (d, J = 8.2 Hz, 1H), 7.78 (d, J = 8.9 Hz, 2H), 7.31 (br s, 1H), 6.95 (d, J = 8.9 Hz, 2H), 6.93 (br s, 1H), 4.41 (m, 1H), 3.73 (t, J = 4.8 Hz, 4H), 3.20 (t, J = 4.8 Hz, 4H), 1.48−1.69 (m, 3H), 0.87 (dd, J = 16, 6.3 Hz, 6H).

To a suspension of *N*^{2}-(4-morpholin-4-ylbenzoyl)leucinamide (**7**) (500 mg, 1 equiv) in toluene (10 mL) were added formaldehyde (0.25 mL of a 37% aq solution, 2 equiv) and 1*H*-1,2,3-benzotriazole (375 mg, 2 equiv). *p*TsOH·H_2O (30 mg, 0.1 equiv) was added, and the resultant suspension was heated to reflux for 2 h with a dean-stark apparatus to remove water. The toluene was then removed using rotary evaporation, and the crude residue was dissolved in diethyl ether and washed with 0.2 N NaOH (3×) and brine (1×), dried, and concentrated. The residue was purified by flash column chromatography on silica gel (gradient elution: 60% EtOAc/hexane to 100% EtOAc) to afford 255 mg (37% yield) of *N*^{1}-(1*H*-1,2,3-benzotriazol-1-ylmethyl)-*N*^{2}-(4-morpholin-4-ylbenzoyl)leucinamide (**8**). ^{1}H NMR (400 MHz, DMSO-d_6) δ 9.37 (t, J = 6.4 Hz, 1H), 8.19 (d, J = 8.33 Hz, 1H), 8.02 (d, J = 8.5 Hz, 1H), 7.93 (d, J = 8.4 Hz, 1H), 7.77 (d, J = 8.8 Hz, 2H), 7.53 (t, J = 7.3 Hz, 1H), 7.39 (t, J = 7.4 Hz, 1H), 6.94 (d, J = 8.9 Hz, 2H), 5.99 (d, J = 6.6 Hz, 2H), 4.47 (m, 1H), 3.73 (t, J = 4.4 Hz, 4H), 3.19 (t, J = 4.4 Hz, 4H), 1.36−1.64 (m, 3H), 0.78 (dd, J = 17, 6.4 Hz, 6H).

To a solution of *N*^{1}-(1*H*-1,2,3-benzotriazol-1-ylmethyl)-*N*^{2}-(4-morpholin-4-ylbenzoyl)leucinamide (**8**) (28.8 mg, 1 equiv) in DMSO-d_6 (0.2 mL) was added Na^{14}CN (4.9 mg from ARC 140A, lot # 980422, 5 mCi). The brown solution was heated to 95 °C for 4 h. EtOAc (40 mL) was added, and the solution was washed with 0.2 N NaOH (6 × 10 mL) and brine (1 × 10 mL), dried, and concentrated to yield 21.1 mg (92% yield) of *N*^{1}-

(C^{14}cyanomethyl)-*N*^{2}-(4-morpholin-4-ylbenzoyl)leucinamide (^{14}C-**9**) which was 95% pure by radioactive reverse phase HPLC. Compound ^{14}C-**9** was purified by flash column chromatography on silica gel (gradient elution: 50% EtOAc/hexanes to 60% EtOAc/hexanes) to provide >99% purity by radioactive reverse phase HPLC (2 mCi). The specific activity of ^{14}C-**9** was 42.6 mCi/mmole.

Confocal Microscopy of HepG2 Cells. HepG2 cells were grown in SlideFlasks in culture media containing MEM Earle's salt supplemented with L-glutamine (Invitrogen); 10% FBS; 1 mM sodium pyruvate; 0.1 mM nonessential amino acids; 100 units/mL penicillin-streptomycin at 37 °C in the presence of 5% CO_2. At 50% confluency, cells were washed with fresh media and then incubated with media containing the test compound added from a 1000-fold stock in DMSO. Control experiments contained only DMSO vehicle. Cells were washed with Hanks's balanced salt solution supplemented with 15 mM HEPES (HHBSS) and then observed by laser scanning microscopy using a Zeiss LSM 510 equipped with an inverted Zeiss Axiovert 100M microscope. Compound **1** (10 μM) was detected using a 2-photon Mira 900 Ti/sapphire (Coherent) laser tuned to 710 nm, with a pulse width of ~3 ps and a repetition rate of 76 MHz. Emitted light was captured with one photomultiplier for wavelengths below 680 nm. To visualize the fluorescent amine Red DND-99 (10 nM), the illumination source was the 543-nm line from a HeNe 1-mW laser passing through the 488/543-nm main dichroic mirror. Fluorescence was recorded using one photomultiplier and a 560-nm long-pass filter. Pinhole and laser intensity were adjusted for the control experiment to avoid saturation of the signal.

Accumulation of ^{14}C-Labeled Cathepsin K Inhibitors within HepG2 Cells. HepG2 cells (grown as above) were seeded in a 96-well Cytostar-T scintillation microplate (Amersham) the day before the experiment and grown as monolayers to ~90% confluency. The cells were washed with 200 μL of HHBSS. Then, 200 μL of HHBSS containing 30 μM of either ^{14}C-**1** (0.02 μCi) or ^{14}C-**9** (0.02 μCi) was added to the cells. Immediately after this addition, the uptake of ^{14}C in to the cells was monitored using a Wallac MicroBeta plate counter. In each well, the radioactivity was read as CPM every 10 min over a 120 min period.

pK_a and Log *P* Measurements. The pK_a and octanol−water partition coefficients were measured using the GLpK_a (Sirius Analytical Instruments) at 25 °C (0.15M KCl, argon) according to the manufacturer's instructions. Potentiometric titrations for **1** and **10** were carried out in dioxane/water and in DMSO/water for **2**. The pK_a measurement for **11** was evaluated in water using a spectroscopic probe. The Log *P* value for **13** was evaluated by the shake flask method described as follows. The partition coefficients were determined by adding 50 μL of the compound dissolved in acetonitrile (2 mg/mL) into 0.75 mL of water and 0.75 mL of 1-octanol which have been mutually saturated with each other. The sample was then vortexed (16000 rpm, 60 s) and allowed to separate (6 h). The concentrations in each phase were determined by HPLC.

Tissue Level Extraction Procedure. Tissue levels were determined by taking a known weight of tissue, adding 2 volumes of water and homogenizing to a frothy suspension using a tissue homogenizer. To this suspension was added 3 volumes of acetonitrile, containing an internal standard. This was then further homogenized, followed by centrifugation (10 min at 14000 rpm). The supernatant was analyzed by LC-MSMS using an internal standard and levels obtained were quantified by comparing them to a standard curve generated by spiking rat plasma with compound following the same procedure as detailed above.

Whole-Body Distribution of ^{14}C-1 in Rats. A solution of **1** (5 mg ^{14}C-**1** (70 μCi) + 5 mg cold **1**/mL of 27% PEG-200/5% dextrose) was injected iv (via the jugular vein), at a dose of 1 mL/kg, into two 300 g female Sprague−Dawley rats. The animals were euthanized 1 h after dosing and frozen immediately in isopentane at −40 °C. Sagittal, 50 μm thick, whole-body sections were taken at −20 °C and thaw-mounted onto Scotch tape and then dried overnight in a vacuum-desiccator at room temperature. ^{14}C-**1** standards were obtained by serial dilution in rat blood. Calibrated drops of the blood/^{14}C-**1** standards were placed on Scotch tape strips, which were dried as above. The simultaneous, quantitative determination of the radioactivity in whole-body sections and standards was carried out using a beta-imager 2000 (Biospace Measures, Paris, France). Data from whole-body sections and standards were collected for 21 h. Data analysis was performed using a [β vision $^+$] software (Biospace Measures).

Mouse Cathepsin S Whole Splenocyte Enzyme Occupancy Assay. Mouse splenocytes were prepared from 8 to 10-week old C57Bl/6 mice spleens in PBS, 2 mM glutamine, 10 mM glucose, and 1% (v/v) FBS using a Medimachine tissue disaggregator (DakoCytomation) with a 50 μm Medicons chamber and passed through a 50 μm Filcons filter. Following red blood cells lysis in 140 mM NH_4Cl, 17 mM Tris-HCl pH 7.5, splenocytes were resuspended in media (RPMI 1640, 10 mM HEPES, pH 7, 1 mM sodium pyruvate, 100 U/mL penicillin, 100 μg/mL streptomycin) at 2.5×10^7 cells/mL. The splenocytes (200 uL) were preincubated with test compound for 60 min at 37 °C in a CO_2 incubator in a 96-well plate. The iodinated probe BIL-DMK[8] (1 nM) was then added for 20 min, the reaction was stopped with 10 μM E−64d for 10 min, and cells were centrifuged at 300*g*. The splenocytes were washed with PBS and labeled proteins separated by 12% Tris-Glycine PAGE and quantified as described.[8]

Mouse Antigen Presentation Assay. The mouse antigen presentation assay was performed using a modification of an established protocol.[30] Briefly, compounds were preincubated with A20μPC cells (A20 cells transfected with PC-specific mIgM, obtained from Dr J. R. Drake, Albany Medical College) in a 96-well plate (1×10^5 cells) for 60 min at 37 °C in a CO_2 incubator in RPMI 1640, 10% FBS, 2 mM glutamine, 50 μM β-mercaptoethanol, and 100 U/mL penicillin, 100 μg/mL streptomycin. DO.11.10 cells (1×10^5) (provided by the National Jewish Medical and Research Center, Denver, CO) and the antigen PC-OVA[30] (30 μg/mL) in a final volume of 200 μL were added. IL-2 sretion into culture media, as measured using a mouse IL-2 ELISA kit (Pierce), was determined following an overnight incubation. IC_{50} values were determined with the SOFTmax Pro software using DMSO as the control for no inhibition.

Acknowledgment. We thank Matthew Zrada and Cynthia Bazin for performing the Log *P* and pK_a analyses and Gregg Wesolowski for performing the bone resorption assays.

References

(1) Lecaille, F.; Kaleta, J.; Bromme, D. Human and parasitic papain-like cysteine proteases: their role in physiology and pathology and recent developments in inhibitor design. *Chem. Rev.* **2002**, *102*, 4459−4488.
(2) Turk, D.; Turk, B.; Turk, V. Papain-like lysosomal cysteine proteases and their inhibitors: drug discovery targets? *Biochem Soc. Symp.* **2003**, *70*, 15−30.
(3) Troen, B. R. The role of cathepsin K in normal bone resorption. *Drug News Perspect.* **2004**, *17*, 19−28.
(4) Robichaud, J.; Bayly, C.; Oballa, R.; Prasit, P.; Mellon, C.; Falgueyret, J. P.; Percival, M. D.; Wesolowski, G.; Rodan, S. B. Rational design of potent and selective NH-linked aryl/heteroaryl cathepsin K inhibitors. *Bioorg. Med. Chem. Lett.* **2004**, *14*, 4291−4295.
(5) Tavares, F. X.; Deaton, D. N.; Miller, L. R.; Wright, L. L. Ketoamide-based inhibitors of cysteine protease, cathepsin K: P3 modifications. *J. Med. Chem.* **2004**, *47*, 5057−5068.
(6) Thompson, S. K.; Halbert, S. M.; DesJarlais, R. L.; Tomaszek, T. A.; Levy, M. A.; Tew, D. G.; Ijames, C. F.; Veber, D. F. Structure-based design of non-peptide, carbohydrazide-based cathepsin K inhibitors. *Bioorg. Med. Chem.* **1999**, *7*, 599−605.
(7) Berger, A. B.; Vitorino, P. M.; Bogyo, M. Activity-based protein profiling: applications to biomarker discovery, in vivo imaging and drug discovery. *Am. J. Pharmacogenom.* **2004**, *4*, 371−381.

(8) Falgueyret, J. P.; Black, W. C.; Cromlish, W.; Desmarais, S.; Lamontagne, S.; Mellon, C.; Riendeau, D.; Rodan, S.; Tawa, P.; Wesolowski, G.; Bass, K. E.; Venkatraman, S.; Percival, M. D. An activity-based probe for the determination of cysteine cathepsin protease activities in whole cells. *Anal. Biochem.* **2004**, *335*, 218−227.
(9) Wang, D.; Li, W.; Pechar, M.; Kopeckova, P.; Bromme, D.; Kopecek, J. Cathepsin K inhibitor-polymer conjugates: potential drugs for the treatment of osteoporosis and rheumatoid arthritis. *Int. J. Pharm.* **2004**, *277*, 73−79.
(10) MacIntyre, A. C.; Cutler, D. J. The potential role of lysosomes in tissue distribution of weak bases. *Biopharm. Drug Dispos.* **1988**, *9*, 513−526.
(11) Ishizaki, J.; Yokogawa, K.; Ichimura, F.; Ohkuma, S. Uptake of imipramine in rat liver lysosomes in vitro and its inhibition by basic drugs. *J. Pharmacol. Exp. Ther.* **2000**, *294*, 1088−1098.
(12) Klein, C. D.; Klingmuller, M.; Schellinski, C.; Landmann, S.; Hauschild, S.; Heber, D.; Mohr, K.; Hopfinger, A. J. Synthesis, pharmacological and biophysical characterization, and membrane-interaction QSAR analysis of cationic amphiphilic model compounds. *J. Med. Chem.* **1999**, *42*, 3874−3888.
(13) Reasor, M. J.; Kacew, S. Drug-induced phospholipidosis: are there functional consequences? *Exp. Biol. Med. (Maywood)* **2001**, *226*, 825−830.
(14) Daniel, W. A.; Wojcikowski, J. The role of lysosomes in the cellular distribution of thioridazine and potential drug interactions. *Toxicol. Appl. Pharmacol.* **1999**, *158*, 115−124.
(15) Ivy, G. O.; Schottler, F.; Wenzel, J.; Baudry, M.; Lynch, G. Inhibitors of lysosomal enzymes: accumulation of lipofuscin-like dense bodies in the brain. *Science* **1984**, *226*, 985−987.
(16) McGrath, M. E.; Palmer, J. T.; Bromme, D.; Somoza, J. R. Crystal structure of human cathepsin S. *Protein Sci.* **1998**, *7*, 1294−1302.
(17) Falgueyret, J. P.; Oballa, R. M.; Okamoto, O.; Wesolowski, G.; Aubin, Y.; Rydzewski, R. M.; Prasit, P.; Riendeau, D.; Rodan, S. B.; Percival, M. D. Novel, nonpeptidic cyanamides as potent and reversible inhibitors of human cathepsins K and L. *J. Med. Chem.* **2001**, *44*, 94−104.
(18) Bryant, C.; Palmer, J. T.; Rydzewski, R. M.; Setti, E.; Tian, Z.; Venkatraman, S.; Wang, D. Novel compounds and compositions as protease inhibitors. WO 00/55126, 1999.
(19) (a) Palmer, J. T.; Bryant, C.; Wang, D.-X.; Davis, D. E.; Setti, E. L.; Rydzewski, R. M.; Venkatraman, S.; Tian, Z.-Q.; Burrill, L. C.; Mendonca, R. V.; Springman, E.; McCarter, J.; Chung, T.; Cheung, H.; McGrath, M.; Somoza, J.; Enriquez, P.; Yu, Z. W.; Strickley, R. M.; Liu, L.; Venuti, M. C.; Percival, M. D.; Falgueyret, J.-P.; Prasit, P.; Oballa, R.; Riendeau, D.; Young, R. N.; Wesolowski, G.; Rodan, S. B.; Johnson, C.; Kimmel, D. B.; Rodan, G Design and Synthesis of Tri-Ring P3 Benzamide-Containing Aminonitriles as Potent, Selective, Orally Effective Inhibitors of Cathepsin K. *J. Med. Chem.* **2005**, *24*, 7520−7534. (b) Missbach, M. Dipeptide Nitrile Cathepsin K Inhibitors, WO 01/58886, 2001.
(20) Robichaud, J.; Oballa, R.; Prasit, P.; Falgueyret, J. P.; Percival, M. D.; Wesolowski, G.; Rodan, S. B.; Kimmel, D.; Johnson, C.; Bryant, C.; Venkatraman, S.; Setti, E.; Mendonca, R.; Palmer, J. T. A novel class of nonpeptidic biaryl inhibitors of human cathepsin K. *J. Med. Chem.* **2003**, *46*, 3709−3727.
(21) Dufour, E.; Storer, A. C.; Menard, R. Peptide aldehydes and nitriles as transition state analogue inhibitors of cysteine proteases. *Biochemistry* **1995**, *34*, 9136−9143.
(22) Lemieux, B.; Percival, M. D.; Falgueyret, J. P. Quantitation of the lysosomotropic character of cationic amphiphilic drugs using the fluorescent basic amine Red DND-99. *Anal. Biochem.* **2004**, *327*, 247−251.
(23) Ishizaki, J.; Yokogawa, K.; Hirano, M.; Nakashima, E.; Sai, Y.; Ohkuma, S.; Ohshima, T.; Ichimura, F. Contribution of lysosomes to the subcellular distribution of basic drugs in the rat liver. *Pharm. Res.* **1996**, *13*, 902−906.
(24) Ishizaki, J.; Yokogawa, K.; Nakashima, E.; Ohkuma, S.; Ichimura, F. Influence of ammonium chloride on the tissue distribution of anticholinergic drugs in rats. *J. Pharm. Pharmacol.* **1998**, *50*, 761−766.
(25) Everts, V.; Hou, W. S.; Rialland, X.; Tigchelaar, W.; Saftig, P.; Bromme, D.; Gelb, B. D.; Beertsen, W. Cathepsin K deficiency in pycnodysostosis results in accumulation of nondigested phagocytosed collagen in fibroblasts. *Calcif. Tissue Int.* **2003**, *73*, 380−386.
(26) Saftig, P.; Hunziker, E.; Wehmeyer, O.; Jones, S.; Boyde, A.; Rommerskirch, W.; Moritz, J. D.; Schu, P.; von Figura, K. Impaired osteoclastic bone resorption leads to osteopetrosis in cathepsin-K-deficient mice. *Proc. Natl. Acad. Sci U. S. A.* **1998**, *95*, 13453−13458.
(27) Honey, K.; Rudensky, A. Y. Lysosomal cysteine proteases regulate antigen presentation. *Nat. Rev. Immunol.* **2003**, *3*, 472−482.
(28) Bryant, C.; Bunin, B. A.; Kraynack, E.; Patterson, J. Novel Compounds and Compositions as Protease Inhibitors. WO 00/55125, 2000.
(29) Shi, G. P.; Villadangos, J. A.; Dranoff, G.; Small, C.; Gu, L.; Haley, K. J.; Riese, R.; Ploegh, H. L.; Chapman, H. A. Cathepsin S required for normal MHC class II peptide loading and germinal center development. *Immunity* **1999**, *10*, 197−206.
(30) Shaw, A. C.; Mitchell, R. N.; Weaver, Y. K.; Campos-Torres, J.; Abbas, A. K.; Leder, P. Mutations of immunoglobulin transmembrane and cytoplasmic domains: effects on intracellular signaling and antigen presentation. *Cell* **1990**, *63*, 381−392.

JM0504961